

Article

Chemical and Biological Study of Novel Aplysiatoxin Derivatives from the Marine Cyanobacterium *Lyngbya* sp.

Hui-Hui Zhang ¹, Xin-Kai Zhang ¹, Ran-Ran Si ², Si-Cheng Shen ¹, Ting-Ting Liang ³, Ting-Ting Fan ¹, Wei Chen ¹, Lian-Hua Xu ^{1,*} and Bing-Nan Han ^{1,*}

¹ Department of Development Technology of Marine Resources, College of Life Sciences and Medicine, Zhejiang Sci-Tech University, Hangzhou 310018, China; huihuizhang09@163.com (H.-H.Z.); xinkaiz2020@163.com (X.-K.Z.); ammashen7@163.com (S.-C.S.); mmfft1994@163.com (T.-T.F.); weichen120903@163.com (W.C.)

² School of Materials Science and Engineering, Zhejiang Sci-Tech University, Hangzhou 310018, China; Siranran95@163.com

³ School of Chemical and Environmental Engineering, Shanghai Institute of Technology, Shanghai 201418, China; liang_tting@163.com

* Correspondence: lianhuaxu@zstu.edu.cn (L.-H.X.); hanbingnan@zstu.edu.cn (B.-N.H.); Tel.: +86-571-8684-3303 (B.-N.H.)

Received: 15 September 2020; Accepted: 20 November 2020; Published: 23 November 2020



Abstract: Since 1970s, aplysiatoxins (ATXs), a class of biologically active dermatotoxins, were identified from the marine mollusk *Stylocheilus longicauda*, whilst further research indicated that ATXs were originally metabolized by cyanobacteria. So far, there have been 45 aplysiatoxin derivatives discovered from marine cyanobacteria with various geographies. Recently, we isolated two neo-debromoaplysiatoxins, neo-debromoaplysiatoxin G (**1**) and neo-debromoaplysiatoxin H (**2**) from the cyanobacterium *Lyngbya* sp. collected from the South China Sea. The freeze-dried cyanobacterium was extracted with liquid–liquid extraction of organic solvents, and then was subjected to multiple chromatographies to yield neo-debromoaplysiatoxin G (**1**) (3.6 mg) and neo-debromoaplysiatoxin H (**2**) (4.3 mg). They were elucidated with spectroscopic methods. Moreover, the brine shrimp toxicity of the aplysiatoxin derivatives representing differential structural classifications indicated that the debromoaplysiatoxin was the most toxic compound (half inhibitory concentration (IC₅₀) value = 0.34 ± 0.036 μM). While neo-aplysiatoxins (neo-ATXs) did not exhibit apparent brine shrimp toxicity, but showed potent blocking action against potassium channel Kv1.5, likewise, compounds **1** and **2** with IC₅₀ values of 1.79 ± 0.22 μM and 1.46 ± 0.14 μM, respectively. Therefore, much of the current knowledge suggests the ATXs with different structure modifications may modulate multiple cellular signaling processes in animal systems leading to the harmful effects on public health.

Keywords: marine cyanobacterium; *Lyngbya* sp.; aplysiatoxin; Kv1.5 inhibitory activity; brine shrimp toxicity

Key Contribution: Two novel aplysiatoxin derivatives were isolated from the marine cyanobacterium *Lyngbya* sp. Neo-debromoaplysiatoxin G (**1**) and neo-debromoaplysiatoxin H (**2**) featuring novel structural skeletons characterized by a bicyclo[2.1.1]tetrahydropyran and unique 5/6 fused-ring systems, respectively. Compounds **1** and **2** showed potent blocking action against potassium channel Kv1.5.

1. Introduction

Marine cyanobacteria, known as blue-green algae, can yield cyanotoxins with many biologically active metabolites, which contained three major groups based largely on their primary toxicological effects: hepatotoxins, neurotoxins, and contact irritants [1,2]. Among them, aplysiatoxins (ATXs), a kind of dermatoxins, which belonged to contact irritants in cyanotoxins, had attracted extensive attentions due to its series of poisoning and allergic events to public health [2–6]. ATXs were first discovered from the digestive gland of the *Stylocheilus longicauda* in 1970s [7,8]. Moreover, further study revealed that these toxins produced from cyanobacteria, which are “prey” of the sea hares [9,10]. Subsequently, ATXs and their related analogues were isolated from *Oscillatoria nigroviridis*, *Schizothrix calcicola*, and *Moorea producens* (formerly *Lyngbya majuscula*), which all belonged to cyanobacterial species [11–14]. In the 1980s, ATXs were confirmed as the factor causing marine dermatitis, because the blooms of *Lyngbya majuscula* broke out on the beach of Oahu Island, Hawaii, with itching or burning, evolving into a blistering eruption [3]. In the 1990s, ATXs and its related compounds led to the causative agents of successive food poisoning cases, with diarrhea, vomiting, and a burning sensation in the throat and mouth [4–6].

ATXs are a class of biologically active dermatoxins with tumor-promoting properties, anti-proliferative activity, antiviral activity, antileukemia activity, and pro-inflammatory actions [11,15–18]. So far, about 45 ATXs were identified from marine cyanobacteria, and mainly existed in *Lyngbya* [19–24]. Thus, the blooms of *Lyngbya* were often concerned with negative impacts on human health and economic implications [25]. In 2018, it was firstly reported that some ATXs exhibit potent blocking action against potassium channel Kv1.5 [20]. The potassium channel Kv1.5 expressed in cardiomyocytes of mammals [26,27], may be one of the key targets resulting in the harmful effects on public health. Based on this, our continuous study aimed to deepen the understanding of ATXs with different structural modifications that may modulate multiple cellular signaling processes in animal systems. In this study, we reported the extraction, structure elucidation, and biological activities of two neo-debromoaplysiatoxins (NEOs) featuring novel structural skeletons, neo-debromoaplysiatoxin G (1) and neo-debromoaplysiatoxin H (2), characterized by a bicyclo[2.1.1]tetrahydropyran and unique 5/6 fused-ring systems, respectively (Figure 1A).

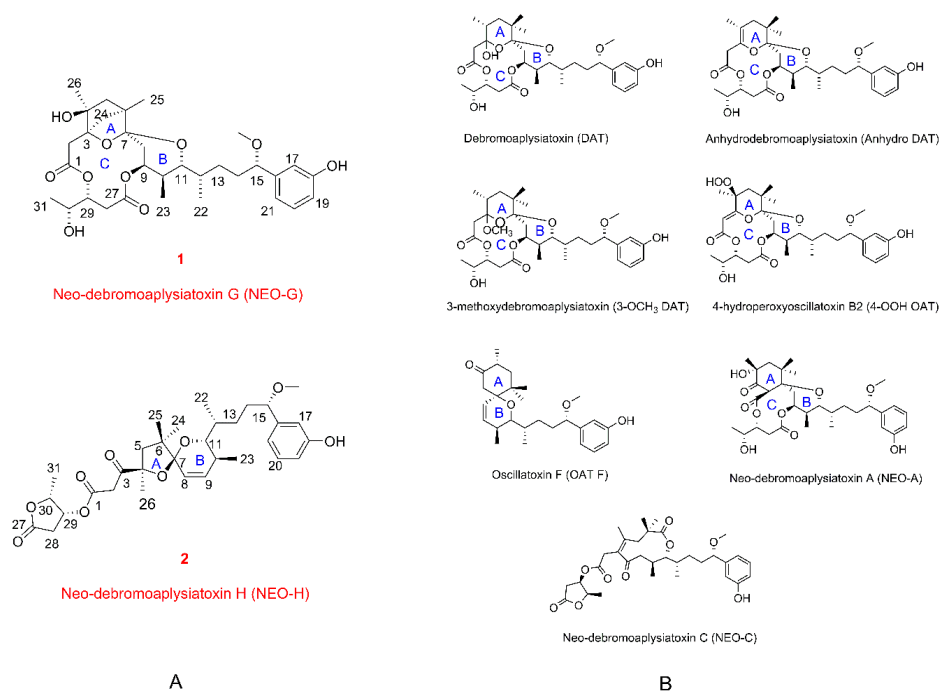


Figure 1. (A) Structures of neo-debromoaplysiatoxin G (1) and neo-debromoaplysiatoxin H (2); (B) structures of reported aplysiatoxin derivatives.

2. Results

The freeze-dried sample of the cyanobacterium was extracted with liquid–liquid extraction of organic solvents. The resultant extracts were subjected to multiple chromatographies to yield neo-debromoaplysiatoxin G (**1**) (3.6 mg), neo-debromoaplysiatoxin H (**2**) (4.3 mg).

2.1. Structure Elucidation of the New Compounds

Neo-debromoaplysiatoxin G (**1**) was a white solid ($[\alpha]_D^{25} + 31.83$ (c 0.07, MeOH); UV (MeOH) λ_{\max} (log ϵ) 217 (4.58), 275 (4.19) nm (Figure S2.9); IR (KBr) ν_{\max} 3854, 3744, 3714, 2960, 1654, 1630, 1587 cm^{-1} (Figure S2.10); High-Resolution Electrospray Ionization Mass Spectroscopy (HRESIMS) data (m/z 613.2984 $[\text{M} + \text{Na}]^+$, calcd 613.2989) (Figure S2.8) assign its molecular formula as $\text{C}_{32}\text{H}_{46}\text{O}_{10}$ with ten degrees of unsaturation. The 32 carbon resonances can be accounted for as eight quaternary carbons, eleven methines, seven methylenes, and six methyls in ^{13}C Nuclear Magnetic Resonance (NMR) (Table 1, Figures S2.1 and S2.2) and Distortionless Enhancement by Polarization Transfer (DEPT) spectra (Figure S2.3). Interpretation of the one-dimensional (1D) and two-dimensional (2D) NMR spectra (Figures S2.4–S2.7) indicated that the planar structure of **1** closely resembles those of aplysiatoxin analogues. Spectroscopic analysis indicated the presence of a side chain attached with a phenol ring at C-16, a methoxy at C-15, and a methyl at C-12 (C-12 to C-22), which was identical to the corresponding portion in ATXs. Heteronuclear Multiple Bond Correlation (HMBC) displayed there was a six-membered ring A connected C-1 (δ C 172.1) with methylene at C-2. Interestingly, HMBC correlations of H₂-24 to C-4, C-5, C-6, C-7, and the slightly downfield chemical shifts of C-6 (δ C 48.7) explained the presence of the bridge ring (C3-C24-C6) on the ring A system. The ^{13}C NMR chemical shifts of C-3 (δ C 85) and C-7 (δ C 105.5) showed having oxide functionalities on the six-membered bridged ring system. C-7 and C-11 were attached to oxide based on the 1D and 2D NMR shift data as well as the structural features of ATXs. Herein, the partially elucidated structure accounted for seven degrees of unsaturation. The ^1H - ^1H Correlation Spectroscopy (COSY) correlations of H₂-28/H-29/H-30/H₃-31 and HMBC correlations of H-28 to C-27 (δ C 171.0), H-29 to C-27, H₃-31 to C-29 (δ C 77.1), and C-30 (δ C 68.6) illustrated the existence of a portion of 3,4-dihydroxyvaleric acid (C-27–C-31), which was connected to C-2 methylene through an ester linkage with C-1 (δ C 172.1) and C-29 (δ C 77.1). According to the NMR data and the molecular formula of compound **1**, there remained one ring closure to complete the 10 degrees of unsaturation. A closer comparison of the NMR data of **1** and debromoaplysiatoxin suggested the presence of tetrahydropyran ring B. Although the ester linkage between C-9 and C-27 was not indicated by the HMBC spectrum, the ^1H and ^{13}C NMR data were strongly supportive of this remaining linkage, accounting for the final degree of unsaturation and thereby completing the closure of ring C. The planar structure of **1** was established with a novel structural skeleton featuring a bridge ring (C3-C24-C6) on the ring A system: bicyclo[2.1.1]tetrahydropyran as depicted in Figure 2. The Nuclear Overhauser Effect Spectroscopy (NOESY) experiment and vicinal coupling constants were utilized to speculate the relative configuration of **1** in Figure 3. The proton coupling constants 3.1 Hz of H-8a/H-9 and H-8b/H-9, as well as NOE correlations of H-9/H-10 and H-10/H₃-23, which indicated H-9/H₃-23 presenting an equatorial orientation on a 6-member ether ring. The H-10 and H-11 were determined as axial protons by the large coupling constant ($J = 10.7$ Hz) of H-10/H-11. The NOE correlation of H-11/H-12 suggested a gauche conformer of H-11/H-12 based on previous aplysiatoxins [20]. The NOE correlation H-29/H-30 and coupling constants in accordance ($J = 4.7$ Hz) of H-29/H-28a, ($J = 7.4$ Hz) of H-29/H-28b with those of aplysiatoxins, demonstrated the stereochemistry of H-29 and H-30 was *syn* relationship [14]. The coupling constants ($J = 8.2, 5.0$ Hz) of H-15 and its chemical shift were similar with those of aplysiatoxins [20]. The absolute stereochemistry of C-3 and C-6 was determined by Gauge-Independent Atomic Orbital (GIAO) NMR shift calculation (Tables S1.4.1 and S1.4.2) followed by DP4⁺ analysis (Table S1.4.4) as isomer 2 (3*S*, 6*R*) with a probability of 100% based on ^1H NMR, ^{13}C NMR (Figure S1.4.1). Furthermore, due to their structural similarities, it was likely that compound **1** had a common biosynthetic origin with previously

reported ATXs [14,20]. Therefore, the absolute stereochemistry was speculated as 3*S*, 4*S*, 6*R*, 9*S*, 10*S*, 11*R*, 12*S*, 15*S*, 29*R*, 30*R*.

Table 1. ¹H (600 MHz) and ¹³C (150 MHz) NMR Data for Compounds **1**, **2** in CDCl₃ (δ in ppm, *J* in Hz).

Pos.	1		2	
	δ _H (<i>J</i> in Hz)	δ _C	δ _H (<i>J</i> in Hz)	δ _C
1		172.1		167.4
2	a 2.72, d (12.6) b 2.69, d (12.6)	34.8	a 4.10, d (16.5) b 3.45, d (16.5)	43.5
3		85		206.5
4		79.2		86.2
5	a 2.02, d (10.5) b 1.84, d (10.5, 2.9)	47.1	a 2.59, d (12.7) b 1.68, d (12.7)	46.4
6		48.7		47.3
7		105.5		106.8
8	a 2.24, dd (14.3, 3.1) b 1.59, dd (14.3, 3.2)	34	5.60, dd (10.2, 2.7)	122.6
9	4.89, m	74.1	5.86, dd (10.2, 2.7)	138.1
10	1.69, m	34	2.16, m	30.0
11	3.86, d (10.7)	74	3.21, overlap	78.7
12	1.52, m	33.9	1.60, overlap	34.6
13	a 1.52, m b 1.41, m	31.3	1.27	29.4
14	a 1.79, m b 1.62, m	37.5	a 1.85, m b 1.60, overlap	36.3
15	4.00, dd (8.2, 5.0)	84.6	3.94, t-like (6.7)	83.5
16		144.7		144
17	6.79, t-like (2.0)	113.5	6.77, overlap	113.9
18		156.3		156.1
19	6.76, ddd (8.0, 2.6, 1.2)	114.7	6.77, overlap	114.6
20	7.22, t-like (8.0)	129.8	7.21, t-like (7.7)	129.7
21	6.86, dt (8.0, 1.2)	118.2	6.83, d (7.4)	118.5
22	0.81, d (6.4)	12.1	0.81, d (6.8)	13.3
23	0.78, d (6.9)	13.6	0.90, d (6.4)	17.0
24	a 2.47, dd (12.9, 2.9) b 1.31, d (12.9)	47.2	0.89, s	23.0
25	1.01, s	15.7	1.09, s	26.3
26	1.41, s	22.3	1.43, s	25.7
27		171		174.3
28	a 2.95, dd (14.8, 4.7) b 2.56, d (14.8, 7.4)	36.3	a 2.92, dd (18.3, 6.1) b 2.70, d (18.3)	36.7
29	4.81, m	77.1	5.51, t-like (5.1)	72.1
30	4.22, m	68.6	4.73, m	79.1
31	1.23, d (6.4)	18.5	1.39, d (6.6)	14.1
15-OCH ₃	3.26, s	57.2	3.21, overlap	56.6

NMR data of debromoaplysiatoxin in Table S3.2 of Supplementary Materials.

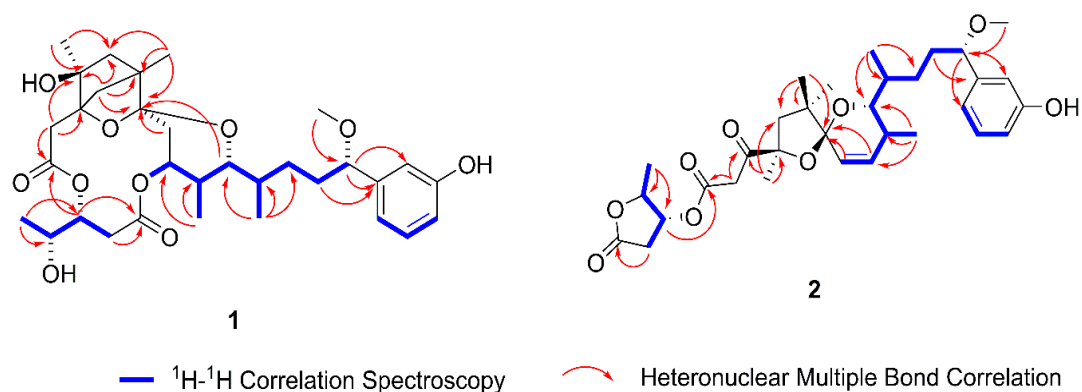


Figure 2. Key ^1H - ^1H Correlation Spectroscopy and Heteronuclear Multiple Bond Correlations of **1** and **2**.

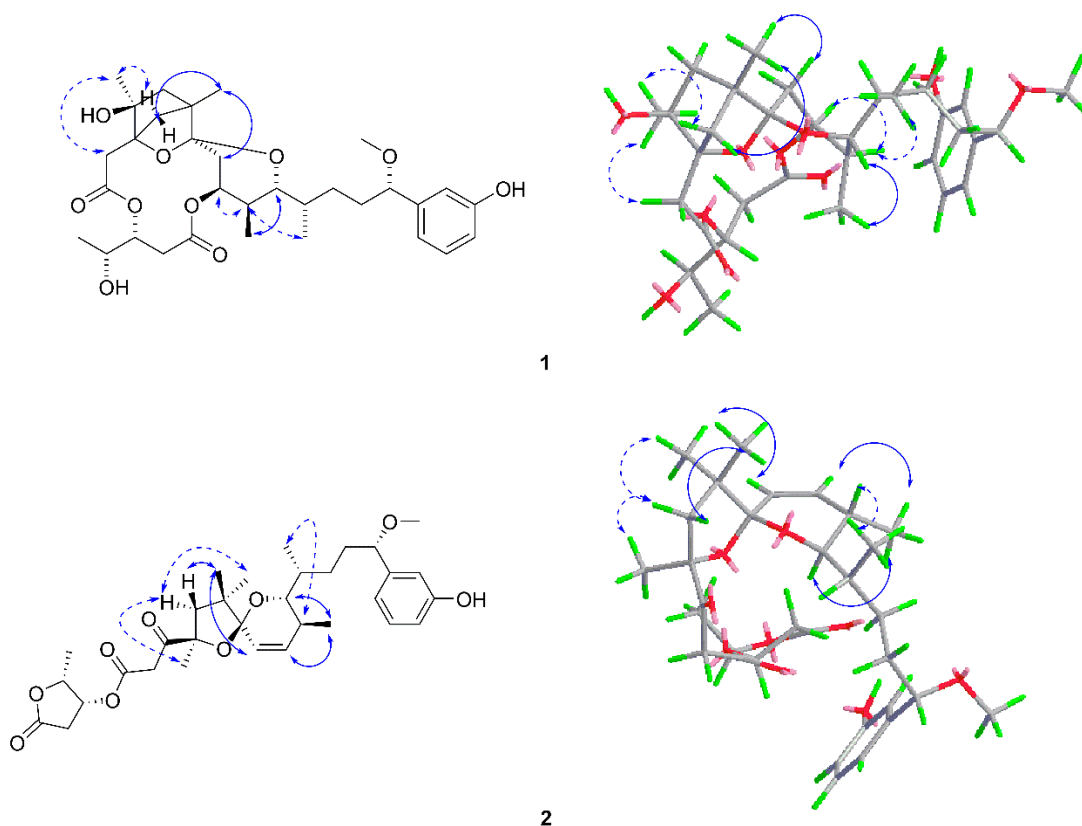


Figure 3. Key Nuclear Overhauser Effect Spectroscopy correlations of **1** and **2** (solid lines: α -orientation; dashed lines: β -orientation).

Neo-debromoaplysiatoxin H (**2**), a colorless solid ($[\alpha]_{\text{D}}^{25} + 31.55$ (c 0.07, MeOH); UV (MeOH) λ_{max} (log ϵ) 217 (4.57), 274 (4.17) nm (Figure S2.19); IR (KBr) ν_{max} 3430, 1654, 1632, 1587, 1561, 1407, 1384 cm^{-1} (Figure S2.20), had a molecular formula of $\text{C}_{32}\text{H}_{44}\text{O}_9$ with 11 degrees of unsaturation as established by the HRESIMS ion peak at m/z 595.2887 ($[\text{M} + \text{Na}]^+$, calcd 595.2985) (Figure S2.18). Its ^{13}C NMR and ^1H NMR spectra (Figures S2.11 and S2.12) exhibited 32 carbon signals and attributed to one methoxy, six methyls, five methylenes, twelve methines, and eight quaternary carbons, including one carbonyl carbon (Table 1). The ^1H NMR spectra and ^{13}C NMR spectra revealed the molecule exhibited a 1, 3-disubstituted benzene ring, which was connected to the side chain at C-15 supported by the HMBC correlations (Figure S2.16) from H-15 to C-17 and C-21. Further, the γ -lactone ring was determined by consecutive ^1H - ^1H COSY correlations (Figure S2.15) combined with the HMBC correlations, where C-27 and C-30 were possibly connected by an ester bond on basis of the ^1H and ^{13}C NMR shift data. The γ -lactone ring was connected to C-1 through an ester linkage with C-1 and C-29 by

the HMBC correlation from H-29 to C-1. The HMBC correlations from H₂-2 to C-1, C-3 established the structure: β -ketone ester. HMBC cross-peaks, as well as the last unsaturation of this molecule explaining the unsaturated two dioxygen spiral ring (5/6) and the ring A (C4-C5-C6-C7), was connected to ring B (C8-C9-C10-C11) through C-7 (δ C 106.8). The C-4 was connected to C-7 and C-7 to C-11 through oxygen atom linkage with C-4 (δ C 86.2), C-7 (δ C 106.8), and C-11 (δ C 78.7). Accordingly, the planar structure of Compound **2** was confirmed (Figure 2), and the novel structural skeleton of neo-debromoaplysiatoxin H (**2**) was characterized with a unique 5/6 fused-dioxygen spiral ring system. The relative configuration of **2** was confirmed by the NOESY spectrum and vicinal coupling constants (Figure S2.17) (Figure 3). The small proton coupling constant (10.2 Hz) indicated an *Z* configuration of $\Delta^{8,9}$. The NOE correlation H₃-26/H-5a/H₃-24 and H-5b/H₃-25 suggested that H-5b/H₃-25 were α -orientation, H₃-26/H-5a/H₃-24 were β -orientation. Due to the NOE correlations of H₃-25/H-8, H-9/H₃-23/H-11, H-10/H₃-22 and an *Z* configuration of $\Delta^{8,9}$, conferred that H₃-23/H-11 were the same orientation, H₃-22 in β -orientation. Because the signals of H-11/H-12 were overlapped with 15-OCH₃ and H-14b, the coupling constants were not able to be obtained, and the relative stereochemistry of H-11/12 of **2** was proposed as 11*R**, 12*S**, with the same relative stereochemistry of **1** based on the same bio-genetics. The coupling constants of H and the chemical shifts of C and H at the γ -lactone ring in **2** were in accordance with those of 30-methylscillatoxin D indicating the same relative configuration of **2** and the known ATXs at C-29 and C-30 [14,22], which established a relative stereochemistry of 29*R** and 30*R**. Therefore, the stereochemistry was speculated as 4*R**, 7*S**, 10*S**, 11*R**, 12*S**, 15*S**, 29*R**, 30*R**.

2.2. Biological Activities of the Isolated Compounds

2.2.1. Inhibitory Activities against Kv1.5

Ultra-rapid delayed rectifier K⁺ current (I_{Kur}) mediated by Kv1.5 is the main current in the repolarization process of cardiomyocyte action potentials, and potent blocking activity against potassium channel Kv1.5 may lead to the harmful effects on public health. In this study, we reported the ATXs isolated from Sanya, China, neo-debromoaplysiatoxin G (**1**) and neo-debromoaplysiatoxin H (**2**), whose inhibitory activities against Kv1.5 were evaluated (Figures S1.3.1.1–S1.3.1.3). Compounds **1** and **2** showed potent dose-response study results with half inhibitory concentration (IC₅₀) values of 1.79 ± 0.22 μ M and 1.46 ± 0.37 μ M, respectively (Figure 4).

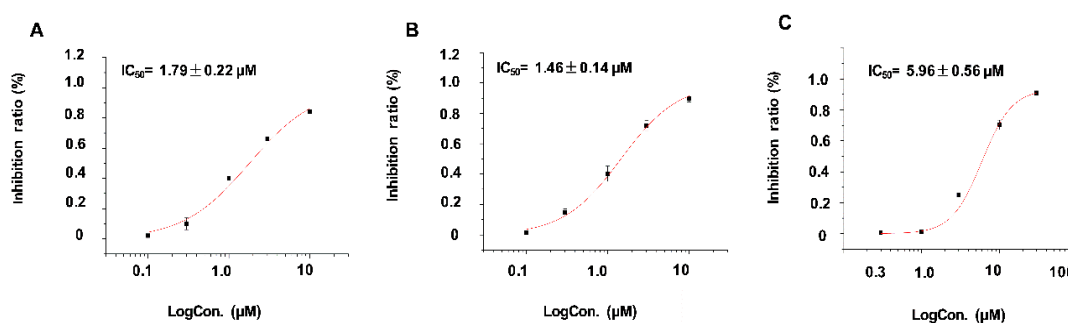


Figure 4. Dose-response study of **1** and **2** with Kv1.5 expression in Chinese hamster ovary (CHO) cells at holding potential (HP) of -80 mV. Data points represent mean \pm SEM of 3 to 5 measurements. Solid curve fits to the Hill equation. (A) The inhibitory effect of **1** showed a half inhibitory concentration (IC₅₀) value of 1.79 \pm 0.22 μ M; (B) The inhibitory effect of **2** showed an IC₅₀ value of 1.46 \pm 0.37 μ M; (C) The inhibitory effect of acetin showed an IC₅₀ value of 5.96 \pm 0.56 μ M.

2.2.2. Toxicity of Brine Shrimp

The investigation of brine shrimp toxicity of nine aplysiatoxin derivatives (debromoaplysiatoxin (DAT), anhydrodebromoaplysiatoxin (Anhydro DAT), 3-methoxydebromoaplysiatoxin (3-OCH₃ DAT), 4-hydroperoxyosciliatoxin B (4-OOH OAT), osciliatoxin F (OAT F), neo-debromoaplysiatoxin A (NEO-A), neo-debromoaplysiatoxin B (NEO-B), neo-debromoaplysiatoxin C (NEO-C), neo-debromoaplysiatoxin G

(NEO-G), neo-debromoaplysiatoxin H (NEO-H) isolated from the same collection (Figure 1B), representing differential structural classifications was conducted. The survival of *Artemia salina* (*A. salina*) began to be influenced by DAT at the concentration as low as 0.1 μM as shown in Figure 5 (Table S1.3.2.1), followed by analogs of DAT (anhydro DAT, 3-OCH₃ DAT) at a concentration of 10 μM . The other ATXs with different structural classifications such as OAT F, Neo-A, and compound 1 and 2 had no apparent effect at 30 μM . As the results indicated, debromoaplysiatoxin was the most toxic compound (IC_{50} value = $0.34 \pm 0.036 \mu\text{M}$) (Figure S1.3.2.2) compared to other tested derivatives, and the 3-hydroxy group at DAT seemed quite important to determine the higher toxicity in comparison to 3-OCH₃ DAT and anhydro DAT, which are dehydroxylated or methylated of 3-hydroxy group at DAT, respectively.

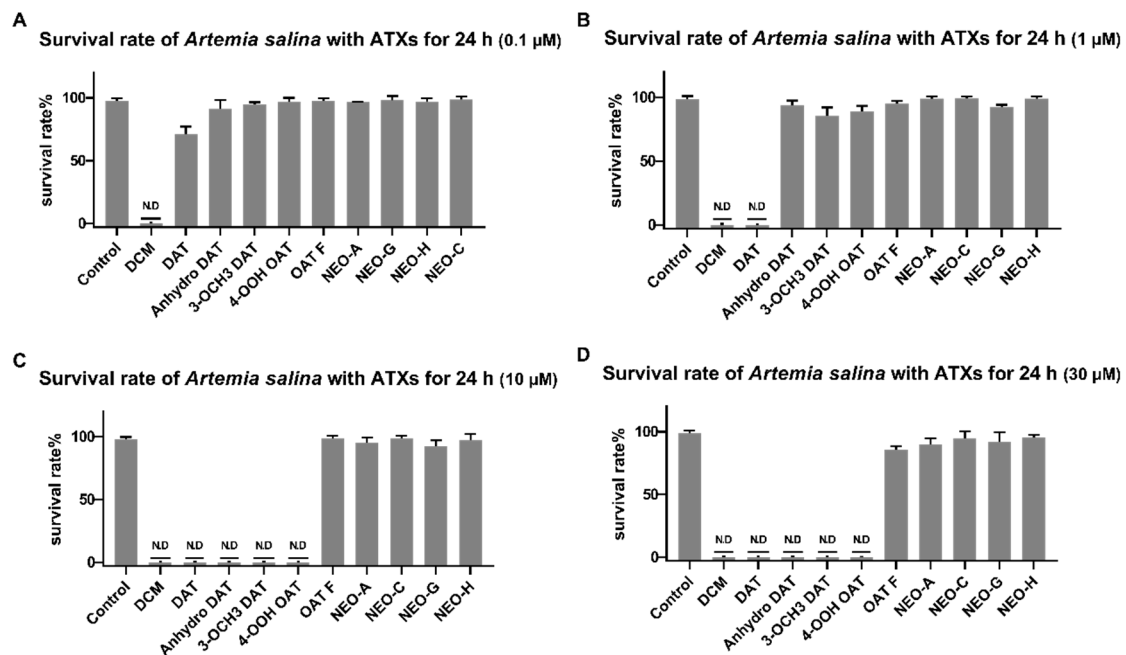


Figure 5. Effect of compound 1 and 2 to *Artemia salina* (*A. salina*). *A. salina* were treated with indicated concentration (0.1 μM , 1 μM , 10 μM , 30 μM) of dichloromethane (DCM), debromoaplysiatoxin (DAT), anhydrodebromoaplysiatoxin (Anhydro DAT), 3-methoxydebromoaplysiatoxin (3-OCH₃ DAT), 4-hydroperoxyosciliatoxin B (4-OOH OAT), osciliatoxin F (OAT F), neo-debromoaplysiatoxin A (NEO-A), neo-debromoaplysiatoxin B (NEO-B), neo-debromoaplysiatoxin C (NEO-C), compound 1 and 2 for 24 h. The percentage of *A. salina* with all different kinds of ATXs. (A) The percentage of *A. salina* with all different kinds of aplysiatoxins (ATXs) in 0.1 μM ; (B) the percentage of *A. salina* with all different kinds of ATXs in 1 μM ; (C) the percentage of survival of *A. salina* with different kinds of ATXs in 10 μM ; (D) the percentage of *A. salina* with all different kinds of ATXs in 30 μM . N.D: not detected the life of brine shrimp. The data were analyzed by GraphPad prism (Table S1.3.2.1).

3. Discussion

Species of *Lyngbya* as the major cyanobacterial species frequently detected from the occurrence of cyanobacterial blooms [28,29], can produce large array toxins, which cause irritant and allergenic responses in human and animal tissues with contact [2,30,31]. ATXs are a kind of dermatotoxins from the marine cyanobacterium *Lyngbya* sp., which have drawn more and more attention due to their structural diversity associated with intriguing biological activities [11,15–18,32]. In this study, we reported the chemical and biological activities of two neo-ATXs along with many known ATXs isolated from this specimen. Based on their structural characteristics, the ATXs were classified into four categories: traditional ATXs with 6/12/6 tricyclic ring systems featuring a macrolactone ring (ABC ring); oscillatoxins featuring a spirobicyclic system (AB ring); nhatrangins with acyclic structure; and the fourth type, intriguing neo-ATXs displaying rare carbon skeletons differing that of traditional ATXs (Figure 1). Analysis of the distribution of 45 aplysiatoxin derivatives discovered across a relatively

broad oceanic area (Figure S3.1, Table S3.1), showed that the traditional ATXs were most commonly detected compared to other ATXs, while the neo-ATXs were only discovered in the cyanobacterial samples from Hainan, China, and Okinawa, Japan. Whether multiple structural rearrangements of the traditional ATXs were caused by environmental stress, climate, water quality, or other factors remains to be further investigated.

In the previous reports, the traditional ATXs, such as ATX and DAT, exhibited multiple biological activities, correlated with skin irritation, diarrhea, antiviral activities, tumor-promoting, anti-proliferative, and pro-inflammatory [11,15–18]. Meanwhile, OAT I showed more potent cytotoxicity and diatom growth inhibition tests compared to the traditional ATXs such as ATX, DAT, 3-OCH₃ DAT, and so on [14,23,33]. Most of neo-ATXs were found to have potent blocking action against potassium channel Kv1.5 (IC₅₀ < 10 μM), in which NEO-B had the strongest inhibitory activity against Kv1.5 (IC₅₀ = 0.30 ± 0.05 μM), and compound 1 and 2 had the similar inhibitory activity with NEO-E/F [20,21,33]. Interestingly, DAT and OAT E were also shown inhibitory activity against Kv1.5 (IC₅₀ = 1.28 ± 0.08 μM, 0.79 ± 0.03 μM, respectively) [33]. In this study, the investigation of brine shrimp toxicity of nine aplysiatoxin derivatives showed that debromoaplysiatoxin was the most toxic compound. It should also be noted that the traditional ATXs displayed much higher activities in brine shrimp toxicity assay than other classified ATXs. Investigation of the correlation between the structure of the different ATX derivatives and their biological activities (cytotoxicity and brine shrimp toxicity) is ongoing.

Some ATXs such as DAT and NEO-A, structurally featuring a protein kinase C (PKC) recognition region (dilactone of ring C) and a conformational control region (6/6 Spiro ketal) [32], were reported to possess strong PKC activation as well as potassium channel Kv1.5 inhibition activities [20,21,34]. While most of neo-ATXs exhibited potent inhibition activities against potassium channel Kv1.5 without showing PKC activation [33], would this be the clue to explore the structure-activity relationship for the cause of lethal brine shrimp toxicity as well as the dermal toxicity of ATXs? Therefore, this work may provide extended information and knowledge for further understanding of ATXs with different structural modifications that may modulate multiple cellular signaling processes in animal systems leading to the harmful effects on public health.

In summary, two novel aplysiatoxin derivatives were isolated from the marine cyanobacterium *Lyngbya* sp. Neo-debromoaplysiatoxin G (1) and neo-debromoaplysiatoxin H (2) featuring novel structural skeletons characterized with a bicyclo[2.1.1]tetrahydropyran, and unique 5/6 fused-dioxygen spiral ring system, respectively. Compounds 1 and 2 showed potent blocking action against potassium channel Kv1.5 with IC₅₀ values of 1.79 ± 0.22 μM and 1.46 ± 0.14 μM, respectively.

4. Materials and Methods

4.1. Material of Marine Cyanobacterium *Lyngbya* sp.

The cyanobacterium *Lyngbya* sp. was collected from the South China Sea in November 2016. The identification results of the samples were shown in Figure S1.1. A voucher specimen numbered as BNH-201606 had been well stored in Zhejiang Sci-Tech University.

4.2. General Experimental Procedures

The UV spectrum was obtained using Thermo UV/EV300 spectrophotometry. Optical rotations were recorded with a JASCO P-2000 polarimeter. ¹H and ¹³C NMR spectra were measured on Agilent 600 MHz instruments using CDCl₃ for chemical shifts. Chemical shifts (δ) were expressed in ppm regarding the solvent peak (H 7.26 and C 77.16). ESIMS and HRTOF-ESIMS data were recorded on Waters Xevo G2-XS QTOF spectrometer (Milford, MA, USA, Waters) after direct infusion. A Waters 1525 series instrument (Milford, MA, USA, Waters) equipped with Waters XBridge Prep C-18 column (5 μm, 10 mm × 250 mm, (Milford, MA, USA, Waters) and a 2998 photodiode array detector (Milford, MA, USA, Waters) was used for the high-performance liquid chromatography (HPLC) separation

(Waters, Milford, MA, USA). Silica gel (200–300) mesh, Yantai Jiangyou Silicone Development Co., Ltd. (Yantai, China) and Sephadex LH-20 (20–150 μm , Pharmacia, NJ, USA) were used for column chromatography. Methanol, chloroform, ethyl acetate, acetone, petroleum ether, and 2-propanol were purchased from Shanghai Chemical Reagents Co. (Shanghai, China). All other materials were of the highest grade available.

4.3. Extraction and Isolation

The freeze-dried powder of the Cyanobacterium (150 g) was extracted with CH_2Cl_2 /MeOH (1:1, *v/v*). The resultant extract was suspended in 1 L of MeOH/ H_2O (9:1, *v/v*) and partitioned with CH_2Cl_2 (3×1 L) to yield the CH_2Cl_2 extract (20 g), which was subjected to vacuum liquid chromatography (VLC) over silica gel using gradients of PE/EtOAc (5:1, 2:1, 1:1, 1:2, 1:5, 0:1, *v/v*) to obtain seven subfractions (F.A–G). F.D (800 mg) was further separated by reversed-phase octadecylsilyl silica (ODS) (10–100% MeCN/ H_2O , 180 min, flow rate 20 mL/min, UV detection at 190 nm) to afford twenty-one subfractions (F.D.1–21). Subsequently, the subfraction F.D.11 (55.4 mg) was purified by preparative HPLC (Waters SunFire Prep C18, 42% MeCN/ H_2O , 8.0 mL/min, UV detection at 190 nm) to yield neo-debromoaplysiatoxin G (**1**) (3.6 mg), subfraction F.D.17 (93.2 mg) was further separated by semi-preparative HPLC (YMC-Pack Pro C18, 85% MeOH/ H_2O , 3.0 mL/min, UV detection at 190 nm) to obtain neo-debromoaplysiatoxin H (**2**) (4.3 mg). Many reported ATXs also were obtained by the same collection (Supplementary Materials 1.2).

4.4. Ion Channel Inhibitory Experiment

Cell preparation: the day before the experiment, digestion of Chinese hamster ovary (CHO) cells (Sigma Chemical Co., St. Louis, MO, USA) with a density of 60–80% by trypsin, and split into some small glass plates, which placed in 35 mm petri dish, then added 10% fetal bovine serum (FBS) (Gibco, CA, USA), and Dulbecco's modified eagle medium (DMEM) (HyClone, Logan, UT, USA) culture medium without P/S was cultured overnight in an incubator [35–37] (Supplementary Materials 1.3.1).

Electrophysiology: the cells were transferred to a perfusion tank and perfused with extracellular fluid. The intracellular fluid (mM) was: K Aspartate, 130; MgCl_2 , 5; EGTA 5; HEPES, 10; Tris-ATP 4; pH 7.2 (KOH titration). The intracellular fluid was stored in small portions in a refrigerator at -80°C and thawed on the day of the experiment. The electrodes were filled with intracellular fluid and drawn with PC-10 (Narishige, Japan). Whole-cell patch-clamp recording, noise is filtered using one-fifth of the sampling frequency. The cells were clamped at -80 mV and then depolarized to 20 mV with a square wave lasting 2 s to obtain $\text{Kv}1.5$ current. This procedure is repeated every 20 s. After it was stabilized, compound **1**, compound **2**, and acacetin were perfused, and when the reaction was stabilized, the strength of the blocking was calculated (Supplementary Materials 1.3.1).

4.5. Brine Shrimp Toxicity Assay

The lethality assay of brine shrimp *A. salina* was developed by Vanhaecke et al. [38]. This assay had also been suggested to evaluate the toxicity of compounds [39–41]. Commercially available *A. salina* or brine shrimp cysts were purchased and cultivated in 3.2% of saline water. Before cultivation, the saline was aerated, and then cysts were kept at room temperature for 24 h. For toxicity screening, hatched larvae were collected and introduced in saline water. Add 0.9% saline water and approximately the same number of larvae 30 per well to make a 96-wells test culture plate. ATXs with 0.1 μM , 1 μM , 10 μM , 30 μM were added to the test culture plate, while the equal volume of dimethyl sulfoxide (DMSO) (Aladdin, Shanghai, China) and dichloromethane (Aladdin, Shanghai, China) were added as blank control test and positive control separately. After 24 h at 25°C , the percent of survival of *A. salina* was calculated (Supplementary Materials 1.3.2).

Supplementary Materials: The following are available online at <http://www.mdpi.com/2072-6651/12/11/0733/s1>, experimental details, Figure S1.1: identification of cyanobacterium; Figure S1.3.1: ion channel experiment; Figure S1.3.2: brine shrimp cytotoxicity assay; Figures S2.1–S2.20: 1D and 2D NMR, HRESIMS, UV and IR spectra of compounds **1** and **2**; Figure S1.4.1 and Tables S1.4.2–S1.4.4: NMR calculation and followed by DP4⁺ analysis of **1**; Figure S3.1 and Table S3.1: the distribution of four types of ATXs in various locations.

Author Contributions: H.-H.Z. performed the experiments for the isolation, structure elucidation, and ion channel inhibitory activity evaluation; and prepared the manuscript; X.-K.Z. performed the part of experiments; S.-C.S. and W.C. performed the 1D and 2D NMR experiments; T.-T.F. and T.-T.L. contributed to part of the structure determination; R.-R.S. contributed to jointly supervised the research; B.-N.H. and L.-H.X. supervised the research work and revised the manuscript. All authors have read and agreed to the published version of the manuscript.

Funding: This work was supported by the National Natural Science Foundation of China (81973233), the National Innovation and Entrepreneurship Training Program for College Students in China (201910338031), the Special Program for Research and Development of Zhejiang Sci-Tech University (2019Y009), and the Scientific Research Foundation of Zhejiang Sci-Tech University (17042058-Y).

Acknowledgments: The authors thank the reviewers whose comments and suggestions helped improve this manuscript, and gratefully acknowledge College of Life Sciences and Medicines, Zhejiang Sci-Tech University.

Conflicts of Interest: The authors declare no conflict of interest.

References

1. Niamien-Ebrottie, J.E.; Bhattacharyya, S.; Deep, P.R.; Nayak, B. Cyanobacteria and cyanotoxins in the World: Review. *Int. J. Appl. Res.* **2015**, *1*, 563–569.
2. Burja, A.M.; Banaigs, B.; Abou-Mansour, E.; Burgess, J.G.; Wright, P.C. Marine cyanobacteria—a prolific source of natural products. *Tetrahedron* **2001**, *57*, 9347–9377.
3. Serdula, M.; Bartolini, G.; Moore, R.E.; Gooch, J.; Wiebenga, N. Seaweed itch on windward Oahu. *Hawaii Med. J.* **1982**, *41*, 200–201.
4. Nagai, H.; Yasumoto, T.; Hokama, Y. Aplysiatoxin and debromoaplysiatoxin as the causative agents of a red alga *Gracilaria coronopifolia* poisoning in Hawaii. *Toxicon Off. J. Int. Soc. Toxinol.* **1996**, *34*, 753–761.
5. Nagai, H.; Yasumoto, T.; Hokama, Y. Manauealides, Some of the Causative Agents of a Red Alga *Gracilaria coronopifolia* Poisoning in Hawaii. *J. Nat. Prod.* **1997**, *60*, 925–928.
6. Nagai, H.; Kan, Y.; Fujita, T.; Sakamoto, B.; Hokama, Y. Manauealide C and Anhydrodebromoaplysiatoxin, Toxic Constituents of the Hawaiian Red Alga, *Gracilaria coronopifolia*. *Biosci. Biotechnol. Biochem.* **1998**, *62*, 1011–1013.
7. Kato, Y.; Scheuer, P.J. Aplysiatoxin and debromoaplysiatoxin, constituents of the marine mollusk *Stylocheilus longicauda* (Quoy and Gaimard, 1824). *J. Am. Chem. Soc.* **1974**, *96*, 2245–2246.
8. Watson, M. Midgut gland toxins of Hawaiian sea hares. I. Isolation and preliminary toxicological observations. *Toxicon Off. J. Int. Soc. Toxinol.* **1973**, *11*, 259–267.
9. Mynderse, J.S.; Moore, R.E.; Kashiwagi, M.; Norton, T.R. Antileukemia activity in the Oscillatoriaceae: Isolation of Debromoaplysiatoxin from *Lyngbya*. *Science* **1977**, *196*, 538–540.
10. Luesch, H.; Harrigan, G.G.; Goetz, G.; Horgen, F.D. The cyanobacterial origin of potent anticancer agents originally isolated from sea hares. *Curr. Med. Chem.* **2002**, *9*, 1791–1806.
11. Moore, R.E.; Blackman, A.J.; Cheuk, C.E.; Mynderse, J.S.; Matsumoto, G.K.; Clardy, J.; Woodard, R.W.; Craig, J.C. Cheminform Abstract: Absolute stereochemistries of the aplysiatoxins and oscillatoxin A. *Cheminform* **1984**, *15*, 2484–2489.
12. Chlipala, G.E.; Pham, H.T.; Nguyen, V.H.; Kronic, A.; Shim, S.H.; Soejarto, D.D.; Orjala, J. Nhatrangins A and B, aplysiatoxin-related metabolites from the marine cyanobacterium *Lyngbya majuscula* from Vietnam. *J. Nat. Prod.* **2010**, *73*, 784–787. [PubMed]
13. Gupta, D.K.; Kaur, P.; Leong, S.T.; Tan, L.T.; Prinsep, M.R.; Chu, J.J. Anti-Chikungunya viral activities of aplysiatoxin-related compounds from the marine cyanobacterium *Trichodesmium erythraeum*. *Mar. Drugs* **2014**, *12*, 115–127. [PubMed]
14. Nagai, H.; Watanabe, M.; Sato, S.; Kawaguchi, M.; Xiao, Y.Y.; Hayashi, K.; Watanabe, R.; Uchida, H.; Satake, M. New aplysiatoxin derivatives from the Okinawan cyanobacterium *Moorea producens*. *Tetrahedron* **2019**, *75*, 2486–2494.

15. Yanagita, R.C.; Kamachi, H.; Kikumori, M.; Tokuda, H.; Suzuki, N.; Suenaga, K.; Nagai, H.; Irie, K. Effects of the methoxy group in the side chain of debromoaplysiatoxin on its tumor-promoting and anti-proliferative activities. *Bioorg. Med. Chem. Lett.* **2013**, *23*, 4319–4323.
16. Kikumori, M.; Yanagita, R.C.; Tokuda, H.; Suzuki, N.; Nagai, H.; Suenaga, K.; Irie, K. Structure-activity studies on the spiroketal moiety of a simplified analogue of debromoaplysiatoxin with antiproliferative activity. *J. Med. Chem.* **2012**, *55*, 5614–5626.
17. Kamachi, H.; Tanaka, K.; Yanagita, R.C.; Murakami, A.; Murakami, K.; Tokuda, H.; Suzuki, N.; Nakagawa, Y.; Irie, K. Structure-activity studies on the side chain of a simplified analog of aplysiatoxin (aplog-1) with anti-proliferative activity. *Bioorg. Med. Chem.* **2013**, *21*, 2695–2702.
18. Suganuma, M.; Fujiki, H.; Tahira, T.; Cheuk, C.; Moore, R.E.; Sugimura, T. Estimation of tumor promoting activity and structure-function relationships of aplysiatoxins. *Carcinogenesis* **1984**, *5*, 315–318.
19. Tidgewell, K.; Clark, B.R.; Gerwick, W.H. The natural products chemistry of cyanobacteria. *Compr. Nat. Prod.* **2010**, *2*, 141–188.
20. Han, B.N.; Liang, T.T.; Keen, L.J.; Fan, T.T.; Zhang, X.D.; Xu, L.; Zhao, Q.; Wang, S.P.; Lin, H.W. Two Marine Cyanobacterial Aplysiatoxin Polyketides, Neo-debromoaplysiatoxin A and B, with K⁺ Channel Inhibition Activity. *Org. Lett.* **2018**, *20*, 578–581.
21. Fan, T.T.; Zhang, H.H.; Tang, Y.H.; Zhang, F.Z.; Han, B.N. Two New Neo-debromoaplysiatoxins—A Pair of Stereoisomers Exhibiting Potent Kv1.5 Ion Channel Inhibition Activities. *Mar. Drugs* **2019**, *17*, 652.
22. Tang, Y.H.; Liang, T.T.; Fan, T.T.; Keen, L.J.; Zhang, X.D.; Xu, L.; Zhao, Q.; Zeng, R.; Han, B.N. Neo-debromoaplysiatoxin C, with new structural rearrangement, derived from debromoaplysiatoxin. *Nat. Prod. Res.* **2020**, *34*, 2151–2156. [[PubMed](#)]
23. Nagai, H.; Sato, S.; Iida, K.; Hayashi, K.; Kawaguchi, M.; Uchida, H.; Satake, M. Oscillatoxin I: A New Aplysiatoxin Derivative, from a Marine Cyanobacterium. *Toxins* **2019**, *11*, 366.
24. Kawaguchi, M.; Satake, M.; Zhang, B.T.; Xiao, Y.Y.; Fukuoka, M.; Uchida, H.; Nagai, H. Neo-Aplysiatoxin A Isolated from Okinawan Cyanobacterium *Moorea Producens*. *Molecules* **2020**, *25*, 457.
25. Taylor, M.S.; Stahl-Timmins, W.; Redshaw, C.H.; Osborne, N.J. Toxic alkaloids in *Lyngbya majuscula* and related tropical marine cyanobacteria. *Harmful Algae* **2014**, *31*, 1–8. [[PubMed](#)]
26. Trapani, J.G.; Korn, S.J. Effect of external pH on activation of the Kv1.5 potassium channel. *Biophys. J.* **2003**, *84*, 195–204. [[PubMed](#)]
27. Heijman, J.; Dobrev, D. Ion channels as part of macromolecular multiprotein complexes: Clinical significance. Ionenkanäle als Teil makromolekularer Multiproteinkomplexe: Klinische Signifikanz. *Herzschrittmacherther. Elektrophysiol.* **2018**, *29*, 30–35.
28. Paul, V.J.; Thacker, R.W.; Banks, K.; Golubic, S. Benthic cyanobacterial bloom impacts the reefs of South Florida (Broward County, USA). *Coral Reefs* **2005**, *24*, 693–697.
29. Tiling, K.; Proffitt, C.E. Effects of *Lyngbya majuscula* blooms on the seagrass *Halodule wrightii* and resident invertebrates. *Harmful Algae* **2017**, *62*, 104–112.
30. Osborne, N.J.; Webb, P.M.; Shaw, G.R. The toxins of *Lyngbya majuscula* and their human and ecological health effects. *Environ. Int.* **2001**, *27*, 381–392.
31. O’Neil, J.M.; Davis, T.W.; Burford, M.A.; Gobler, C.J. The rise of harmful cyanobacteria blooms: The potential roles of eutrophication and climate change. *Harmful Algae* **2012**, *14*, 313–334.
32. Ashida, Y.; Yanagita, R.C.; Takahashi, C.; Kawanami, Y.; Irie, K. Binding mode prediction of aplysiatoxin, a potent agonist of protein kinase C, through molecular simulation and structure-activity study on simplified analogs of the receptor-recognition domain. *Bioorg. Med. Chem.* **2016**, *24*, 4218–4227. [[PubMed](#)]
33. Tang, Y.H.; Wu, J.; Fan, T.T.; Zhang, H.H.; Gong, X.X.; Cao, Z.Y.; Zhang, J.; Lin, H.W.; Han, B.N. Chemical and biological study of aplysiatoxin derivatives showing inhibition of potassium channel Kv1.5. *RSC Adv.* **2019**, *9*, 7594–7600.
34. Horowitz, A.D.; Fujiki, H.; Weinstein, I.B.; Jeffrey, A.; Okin, E.; Moore, R.E.; Sugimura, T. Comparative effects of aplysiatoxin, debromoaplysiatoxin, and teleocidin on receptor binding and phospholipid metabolism. *Cancer Res.* **1983**, *43*, 1529–1535. [[PubMed](#)]
35. Yu, J.; Park, M.H.; Jo, S.H. Inhibitory effects of cortisone and hydrocortisone on human Kv1.5 channel currents. *Eur. J. Pharmacol.* **2015**, *746*, 158–166. [[PubMed](#)]
36. Jeong, I.; Yoon, S.H.; Hahn, S.J. Effects of dapoxetine on cloned Kv1.5 channels expressed in CHO cells. *Naunyn-Schmiedeberg’s Arch. Pharmacol.* **2012**, *385*, 707–716.

37. Choi, B.H.; Choi, J.S.; Jeong, S.W.; Hahn, S.J.; Yoon, S.H.; Jo, Y.H.; Kim, M.S. Direct block by bisindolylmaleimide of rat Kv1.5 expressed in Chinese hamster ovary cells. *J. Pharmacol. Exp. Ther.* **2000**, *293*, 634–640.
38. Vanhaecke, P.; Persoone, G.; Claus, C.; Sorgeloos, P. Proposal for a short-term toxicity test with artemia nauplii. *Ecotoxicol. Environ. Saf.* **1981**, *5*, 382–387.
39. Lopes, V.R.; Fernández, N.; Martins, R.F.; Vasconcelos, V. Primary screening of the bioactivity of brackishwater cyanobacteria: Toxicity of crude extracts to *Artemia salina* larvae and *Paracentrotus lividus* embryos. *Mar. Drugs* **2010**, *8*, 471–482.
40. Moshafi, M.H.; Sharififar, F.; Dehghan, G.; Ameri, A. Bioassay screening of the essential oil and various extracts of fruits of *Heracleum persicum* Desf. and Rhizomes of *Zingiber officinale* Rosc. using brine shrimp cytotoxicity assay. *Iran. J. Pharm. Res.* **2009**, *8*, 59–63.
41. Manilal, A.; Sujith, S.; Kiran, G.S.; Selvin, J.; Shakir, C. Cytotoxic potentials of red alga, *Laurencia brandenii* collected from the Indian coast. *Glob. J. Pharmacol.* **2009**, *3*, 90–94.

Publisher’s Note: MDPI stays neutral with regard to jurisdictional claims in published maps and institutional affiliations.



© 2020 by the authors. Licensee MDPI, Basel, Switzerland. This article is an open access article distributed under the terms and conditions of the Creative Commons Attribution (CC BY) license (<http://creativecommons.org/licenses/by/4.0/>).